

Model Predictive Control of Thermo-Hydraulic Systems Using Primal Decomposition ^{*}

Jonathan Vieth ^{*} Annika Eichler ^{**,**} Arne Speerforck ^{*}

^{*} *Institute of Engineering Thermodynamics, Hamburg University of Technology, Denickestraße 17, 21073 Hamburg, Germany (e-mail: jonathan.vieth@tuhh.de, arne.speerforck@tuhh.de).*

^{**} *Institute of Control Systems, Hamburg University of Technology, Hamburg, Germany (e-mail: annika.eichler@tuhh.de)*

^{***} *Deutsches Elektronen-Synchrotron DESY, Hamburg, Germany (e-mail: annika.eichler@desy.de)*

Abstract: Decarbonizing the global energy supply requires more efficient heating and cooling systems. Model predictive control enhances the operation of cooling and heating systems but depends on accurate system models, often based on control volumes. We present an automated framework including time discretization to generate model predictive controllers for such models. To ensure scalability, a primal decomposition exploiting the model structure is applied. The approach is validated on an underground heating system with varying numbers of states, demonstrating the primal decomposition’s advantage regarding scalability.

Keywords: Model predictive control, Thermal systems modeling, Large-scale and networked optimization problems, Primal decomposition, Control and optimization for sustainability and energy systems, Energy management systems, Urban energy distribution systems

1. INTRODUCTION

The European Commission (2019) mandates that building heat supply in the EU must be decarbonized by 2050. A study by Fraunhofer ISE (2021) indicates that the share of buildings heated by district heating networks (DHNs) in Germany must increase to meet climate targets, aligning with Lund et al. (2010). To meet the climate targets, DHNs must be decarbonized. Decarbonizing DHNs requires improving efficiency through strategies like intelligent operation, see Lund et al. (2014). Additionally, cooling demand is the fastest-growing energy use globally; efficiency measures could reduce related electricity costs by about 38% compared to baseline scenarios, according to IEA (2018). In summary, the need for efficiency measures in heating and cooling systems will grow significantly.

Efficiency can be improved through optimized planning and operations. Maurer et al. (2023) study optimal DHN operation using model predictive control (MPC), while Wack et al. (2023) address DHN planning. Deng et al. (2017) apply optimization to district heating and cooling networks, which combine heat and cooling supply using soil as natural storage. Taheri et al. (2022) review MPC for heating, ventilation, and air conditioning systems, highlighting its growing attention recently.

All these systems share two features: they can be modeled using control volumes (CVs), and fluid typically circulates

in pipes to transport energy. Westphal et al. (2025) present a simulation library for DHNs. This library is used by Vieth et al. (2025) for optimal DHN planning. Maurer et al. (2021) compare pipe models for DHN MPC, concluding that CV-based models are preferable due to simplicity and a fixed number of variables, unlike the Node Method by Benonysson (1991). However, CV models result in systems described by time-continuous differential-algebraic equations (DAEs).

Automated approaches for MPC generation for time-continuous DAEs are presented in Fabien (2010), Houska et al. (2011), and Chen et al. (2019). In Fabien (2010), the optimal control problem is solved using a direct method. According to Olanrewaju and Maciejowski (2017), in direct methods first the time-continuous DAEs are time-discretized, and then an optimization problem is solved based on the discretized system model. In contrast, the approaches presented by Houska et al. (2011) and Chen et al. (2019) employ multiple shooting techniques to solve the optimal control problem based on the continuous system model.

This work presents a direct method for thermo-hydraulic systems modeled by CVs. Although time discretization of nonlinear systems is challenging, performing it beforehand can improve computational efficiency. Focusing on thermo-hydraulic systems also enables exploiting their specific model structure through primal decomposition.

Contribution In this work, we present an automated workflow for MPC generation consisting of a general dy-

^{*} This research is supported by the German federal ministry of economic affairs and climate action (BMWK) under the agreement no. 03EWR007O2.

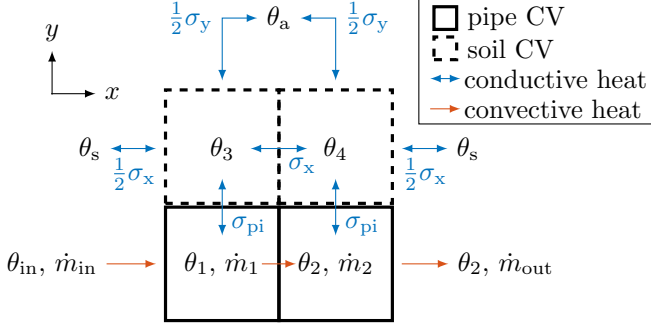


Fig. 1. Simple setup of CVs

dynamic system model for thermo-hydraulic systems (Section 2), a procedure for time discretization of nonlinear dynamic systems based on Backward-Differentiation (Section 3), and a fast and scalable MPC approach for thermo-hydraulic systems using primal decomposition (Section 4).

Notation The identity matrix with n rows and columns is represented by \mathbf{I}_n and $\mathbf{1}_{n \times m}$ is a matrix with n rows and m columns where all elements are equal to one. Vectors are denoted by lowercase bold letters, and matrices by uppercase bold letters.

2. DYNAMICS OF SYSTEMS MODELED BY CONTROL VOLUMES

Consider the system shown in Figure 1, which could represent any type of heating or cooling system. The differential equations (DEs)

$$\frac{d\boldsymbol{\theta}}{dt} = \mathbf{A}\boldsymbol{\theta} + \mathbf{D}\mathbf{d} + \mathbf{X}_\theta [\dot{\mathbf{m}} \circ (\mathbf{Z}_\theta \boldsymbol{\theta})] + \mathbf{X}_z [\mathbf{Y}_z \dot{\mathbf{m}} \theta_{in}] \quad (1a)$$

describe the temperatures $\boldsymbol{\theta}^\top = [\theta_1 \ \theta_2 \ \theta_3 \ \theta_4]$ and the mass flows $\dot{\mathbf{m}}^\top = [\dot{m}_1 \ \dot{m}_2]$ in the CVs. The vector $\mathbf{d}^\top = [\theta_s \ \theta_a]$ comprises the non-controllable inputs: the soil temperature θ_s and the air temperature θ_a . Here, the input temperature θ_{in} is assumed to be an algebraic state (later denoted by z), as in many heating or cooling systems it would be linked with θ_2 and an input variable via an algebraic equation. The constant matrices in (1a) are

$$\mathbf{A} = \begin{bmatrix} -\frac{\sigma_{pi}}{c_w \rho_w V} & 0 & \frac{\sigma_{pi}}{c_w \rho_w V} & 0 \\ 0 & -\frac{\sigma_{pi}}{c_w \rho_w V} & 0 & \frac{\sigma_{pi}}{c_w \rho_w V} \\ \frac{\sigma_{pi}}{c_s \rho_s V} & 0 & -\frac{\sigma_{pi} + \frac{3}{2}\sigma_x + \frac{1}{2}\sigma_y}{c_s \rho_s V} & \frac{\sigma_x}{c_s \rho_s V} \\ 0 & \frac{\sigma_{pi}}{c_s \rho_s V} & \frac{\sigma_x}{c_s \rho_s V} & -\frac{\sigma_{pi} + \frac{3}{2}\sigma_x + \frac{1}{2}\sigma_y}{c_s \rho_s V} \end{bmatrix},$$

$$\mathbf{D} = \frac{1}{2} \begin{bmatrix} 0 & 0 \\ 0 & 0 \\ \frac{\sigma_x}{c_s \rho_s V} & \frac{\sigma_y}{c_s \rho_s V} \\ \frac{\sigma_x}{c_s \rho_s V} & \frac{\sigma_y}{c_s \rho_s V} \end{bmatrix}, \mathbf{X}_\theta = \begin{bmatrix} \frac{1}{\rho_w V} & 0 \\ 0 & \frac{1}{\rho_w V} \\ 0 & 0 \\ 0 & 0 \end{bmatrix}, \mathbf{X}_z = \begin{bmatrix} \frac{1}{\rho_w V} \\ 0 \\ 0 \\ 0 \end{bmatrix},$$

$$\mathbf{Z}_\theta = \begin{bmatrix} -1 & 0 & 0 & 0 \\ 1 & -1 & 0 & 0 \end{bmatrix}, \mathbf{Y}_z = [1 \ 0].$$

Here, V is the volume of each CV, σ_x , σ_y , and σ_{pi} are thermal conductivities, and c_i and ρ_i are the heat capacity and density of the soil (s) and the water (w) inside the pipe, respectively, all considered as constant, as commonly done for MPCs (e.g. Maurer et al. (2023)) and simulation models (e.g. Westphal et al. (2025)). In (1a), we assume that changes in enthalpy due to changes in

pressure are negligible, a condition that is generally met for the systems under consideration. Additionally, algebraic equations (AEs)

$$\dot{m}_{in} = \dot{m}_1 = \dot{m}_2 = \dot{m}_{out} \quad (1b)$$

connect the mass flow variables. Note that inserting (1b) into (1a) would simplify (1a). However, the structure of (1a) leads us to the DAE system

$$\frac{d\boldsymbol{\theta}}{dt} = \mathbf{A}\boldsymbol{\theta} + \mathbf{B}\mathbf{u} + \mathbf{C}\mathbf{z} + \mathbf{D}\mathbf{d} + \sum_{v \in \mathcal{V}} \mathbf{X}_v [(\mathbf{Y}_v \dot{\mathbf{m}}) \circ (\mathbf{Z}_v \mathbf{v})], \quad (2a)$$

$$\mathbf{0} = \mathbf{f}_h(\dot{\mathbf{m}}, \mathbf{z}_h, \mathbf{u}_h, \mathbf{d}), \quad \mathbf{0} = \mathbf{f}_t(\boldsymbol{\theta}, \dot{\mathbf{m}}, \mathbf{z}, \mathbf{u}, \mathbf{d}), \quad (2b)$$

$$\mathbf{0} \geq \mathbf{g}_h(\dot{\mathbf{m}}, \mathbf{z}_h, \mathbf{u}_h, \mathbf{d}), \quad \mathbf{0} \geq \mathbf{g}_t(\boldsymbol{\theta}, \dot{\mathbf{m}}, \mathbf{z}, \mathbf{u}, \mathbf{d}), \quad (2c)$$

which represents an arbitrary system of interconnected CVs with the controllable inputs $\mathbf{u}^\top = [\mathbf{u}_h^\top \ \mathbf{u}_t^\top]$ and the algebraic variables $\mathbf{z}^\top = [\mathbf{z}_h^\top \ \mathbf{z}_t^\top]$. The subscript h denotes variables related to the hydraulics and t to the thermal-model. All matrices are constant, \mathbf{f}_h is a function representing the hydraulic AEs, \mathbf{f}_t all other AEs, \mathbf{g}_h the hydraulic inequality constraints, \mathbf{g}_t all other inequality constraints, and $\mathcal{V} = \{\boldsymbol{\theta}, \mathbf{z}, \mathbf{u}, \mathbf{d}\}$. The reason for extracting the hydraulic constraints from the other constraints is solely for notational purposes and does not lead to any modeling restrictions, since all variables can occur in \mathbf{f}_t and \mathbf{g}_t . This approach is motivated by the primal decomposition scheme, as discussed in Section 4.2.

3. TIME DISCRETIZATION OF SYSTEMS MODELED BY CONTROL VOLUMES

This section aims to derive a time-discrete representation of (2a). Common nonlinear system discretization methods include Taylor approximation (Kazantzis and Kravaris (1999)), Runge-Kutta integration (Herty et al. (2013); Frey et al. (2024)), and backward differentiation (Vaclavek and Blaha (2013)). As shown in Vaclavek and Blaha (2013), Taylor and Runge-Kutta methods can introduce complex nonlinear terms, potentially altering the original structure of (2a) and making the system non-bilinear as the discretization order increases. This increases MPC optimization complexity and eliminates the possibility of linear problems via primal decomposition if nonlinear equations that are not bilinear result from the time-discretization approach.

For this reason, second-order backward differentiation is used. According to Alikhani et al. (2016), the time-discrete system dynamics are given by

$$\mathbf{0} = \mathbf{f}_{de,k}(\boldsymbol{\theta}_k, \dot{\mathbf{m}}_k, \mathbf{z}_k, \mathbf{u}_k, \mathbf{d}_k)$$

$$= \left[\mathbf{I}_{|\boldsymbol{\theta}_k|} - \frac{2}{3}\Delta t \mathbf{A} \right] \boldsymbol{\theta}_k - \frac{4}{3}\boldsymbol{\theta}_{k-1} + \frac{1}{3}\boldsymbol{\theta}_{k-2}$$

$$- \frac{2}{3}\Delta t \left[\mathbf{B}\mathbf{u}_k + \mathbf{C}\mathbf{z}_k + \mathbf{D}\mathbf{d}_k \right] \quad (3)$$

$$+ \sum_{v \in \mathcal{V}} \mathbf{X}_v [(\mathbf{Y}_v \dot{\mathbf{m}}_k) \circ (\mathbf{Z}_v \mathbf{v}_k)]$$

with the constant timestep Δt . Note that the implementation of higher-order backward differentiation is similar.

4. PRIMAL-DECOMPOSITION OF SYSTEMS MODELED BY CONTROL VOLUMES

4.1 General MPC optimization problem

The goal of the MPC is to minimize an objective function

$$J_k \left(\hat{\boldsymbol{\theta}}_k, \hat{\mathbf{m}}_k, \hat{\mathbf{z}}_k, \hat{\mathbf{u}}_k \right) = J_{h,k} \left(\hat{\mathbf{m}}_k, \hat{\mathbf{z}}_{h,k}, \hat{\mathbf{u}}_{h,k} \right) + J_{t,k} \left(\hat{\boldsymbol{\theta}}_k, \hat{\mathbf{m}}_k, \hat{\mathbf{z}}_k, \hat{\mathbf{u}}_k \right), \quad (4a)$$

with the notation convention

$$\hat{\mathbf{a}}_k = [\mathbf{a}_k^\top \mathbf{a}_{k+1}^\top \cdots \mathbf{a}_{k+n_c-1}^\top]^\top,$$

and with

$$J_{h,k} \left(\hat{\mathbf{m}}_k, \hat{\mathbf{z}}_{h,k}, \hat{\mathbf{u}}_{h,k} \right) = \sum_{\kappa \in \mathcal{K}} j_{h,\kappa} \left(\hat{\mathbf{m}}_\kappa, \mathbf{z}_{h,\kappa}, \mathbf{u}_{h,\kappa} \right), \quad (4b)$$

$$J_{t,k} \left(\hat{\boldsymbol{\theta}}_k, \hat{\mathbf{m}}_k, \hat{\mathbf{z}}_k, \hat{\mathbf{u}}_k \right) = \sum_{\kappa \in \mathcal{K}} j_{t,\kappa} \left(\boldsymbol{\theta}_\kappa, \hat{\mathbf{m}}_\kappa, \mathbf{z}_\kappa, \mathbf{u}_\kappa \right) \quad (4c)$$

over all time-steps $\mathcal{K} = \{k, k+n_c-1\}$ within the control-horizon n_c with respect to the hydraulic constraints

$$\mathbf{f}_{h,\kappa}(\hat{\mathbf{m}}_\kappa, \mathbf{z}_{h,\kappa}, \mathbf{u}_{h,\kappa}, \mathbf{d}_\kappa) = 0, \quad \forall \kappa \in \mathcal{K}, \quad (5a)$$

$$\mathbf{g}_{h,\kappa}(\hat{\mathbf{m}}_\kappa, \mathbf{z}_{h,\kappa}, \mathbf{u}_{h,\kappa}, \mathbf{d}_\kappa) \leq 0, \quad \forall \kappa \in \mathcal{K}, \quad (5b)$$

and the non-hydraulic constraints

$$\mathbf{f}_{de,\kappa}(\boldsymbol{\theta}_\kappa, \hat{\mathbf{m}}_\kappa, \mathbf{z}_\kappa, \mathbf{u}_\kappa, \mathbf{d}_\kappa) = 0, \quad \forall \kappa \in \mathcal{K}, \quad (6a)$$

$$\mathbf{f}_{t,\kappa}(\boldsymbol{\theta}_\kappa, \hat{\mathbf{m}}_\kappa, \mathbf{z}_\kappa, \mathbf{u}_\kappa, \mathbf{d}_\kappa) = 0, \quad \forall \kappa \in \mathcal{K}, \quad (6b)$$

$$\mathbf{g}_{t,\kappa}(\boldsymbol{\theta}_\kappa, \hat{\mathbf{m}}_\kappa, \mathbf{z}_\kappa, \mathbf{u}_\kappa, \mathbf{d}_\kappa) \leq 0, \quad \forall \kappa \in \mathcal{K}. \quad (6c)$$

Note that splitting the objective into a hydraulic objective j_h and a temperature objective j_t does not impose any restrictions, since all optimization variables can still be part of j_t . Therefore, the optimization problem that must be solved at each time-step k is given by

$$J_k^* = \min_{\hat{\boldsymbol{\theta}}_k, \hat{\mathbf{m}}_k, \hat{\mathbf{z}}_k, \hat{\mathbf{u}}_k} J_k \left(\hat{\boldsymbol{\theta}}_k, \hat{\mathbf{m}}_k, \hat{\mathbf{z}}_k, \hat{\mathbf{u}}_k \right) \quad \text{subject to (5) and (6),} \quad (7)$$

where J_k^* is the optimal function value of (4a).

4.2 Primal decomposition

As can be seen in (3), assuming $\hat{\mathbf{m}}_k$ is constant makes (3) a linear system of equations. If the same holds true for (2b)–(2c), then *primal decomposition* can be used to efficiently solve the optimization problem (7). Figure 2 displays a procedure of the primal decomposition scheme.

First, a feasible starting point is calculated by solving the system of nonlinear equations (5) and (6), where the control variables are taken from the MPC results of the previous time-step. The algorithm works by iteratively altering $\hat{\mathbf{m}}_k$. The first step in each iteration is to solve the hydraulic optimization problem

$$J_{h,k}^i = \min_{\hat{\mathbf{z}}_{h,k}^i, \hat{\mathbf{u}}_{h,k}^i} J_{h,k} \left(\hat{\mathbf{m}}_k^i, \hat{\mathbf{z}}_{h,k}^i, \hat{\mathbf{u}}_{h,k}^i \right) \quad \text{subject to (5)} \quad (8)$$

with i being the primal decomposition iteration index. Solving (8) yields the optimal values for $\hat{\mathbf{z}}_{h,k}^i$ and $\hat{\mathbf{u}}_{h,k}^i$.

Next, the thermal optimization problem

$$J_{t,k}^i = \min_{\boldsymbol{\theta}_k, \hat{\mathbf{z}}_{t,k}^i, \hat{\mathbf{u}}_{t,k}^i} J_{t,k} \left(\boldsymbol{\theta}_k, \hat{\mathbf{m}}_k^i, \hat{\mathbf{z}}_{h,k}^i, \hat{\mathbf{z}}_{t,k}^i, \hat{\mathbf{u}}_{h,k}^i, \hat{\mathbf{u}}_{t,k}^i \right) \quad \text{subject to (6)} \quad (9)$$

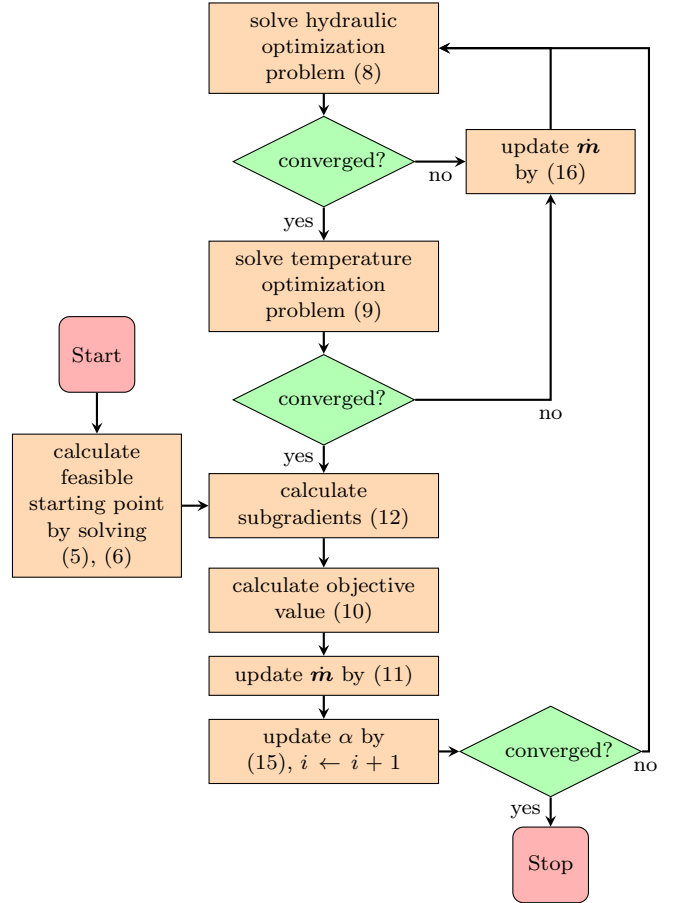


Fig. 2. Procedure of the primal decomposition scheme

is solved, resulting in $\boldsymbol{\theta}_k^i$, $\hat{\mathbf{z}}_{t,k}^i$, and $\mathbf{u}_{t,k}^i$. The objective value after iteration i is given by

$$J_k^i = J_{h,k}^i + J_{t,k}^i. \quad (10)$$

A convergence criterion, e.g. based on $\Delta J = J_k^i - J_k^{i-1}$, can then be used. If the convergence criterion is not met, the primal variable is updated by Boyd et al. (2008)

$$\hat{\mathbf{m}}_k^{i+1} = \hat{\mathbf{m}}_k^i - \alpha^i \mathbf{s}_k^i \quad (11)$$

with the subgradient

$$\mathbf{s}_k = \frac{\partial L_k \left(\hat{\boldsymbol{\theta}}_k, \hat{\mathbf{m}}_k, \hat{\mathbf{z}}_k, \hat{\mathbf{u}}_k, \hat{\boldsymbol{\lambda}}_k \right)}{\partial \hat{\mathbf{m}}_k}, \quad (12)$$

the Lagrangian as in Palomar and Chiang (2006)

$$L_k = J_k - \sum_{\kappa \in \mathcal{K}} \sum_{\mathbf{h} \in \mathcal{H}} \boldsymbol{\lambda}_{h,\kappa}^\top \mathbf{h}_\kappa, \quad (13)$$

the set of constraint functions $\mathcal{H} = \{\mathbf{f}_h, \mathbf{g}_h, \mathbf{f}_{de}, \mathbf{f}_t, \mathbf{g}_t\}$, and the optimal Lagrange multipliers

$$\hat{\boldsymbol{\lambda}}_k^\top = \left[\hat{\boldsymbol{\lambda}}_{f_h,k}^\top \hat{\boldsymbol{\lambda}}_{g_h,k}^\top \hat{\boldsymbol{\lambda}}_{f_{de},k}^\top \hat{\boldsymbol{\lambda}}_{f_t,k}^\top \hat{\boldsymbol{\lambda}}_{g_t,k}^\top \right]. \quad (14)$$

Once again the notation convention from (4) is used, e.g. $\hat{\boldsymbol{\lambda}}_{f_h,k}^\top = [\boldsymbol{\lambda}_{f_h,k}^\top \cdots \boldsymbol{\lambda}_{f_h,k+n_c-1}^\top]$. At the end of each iteration, α^i is updated using the nonsummable, diminishing step-size rule Boyd (2014)

$$\alpha^i = \frac{\alpha}{\sqrt{i}} \quad (15)$$

which is in accordance with the conditions specified in Bertsekas and Tsitsiklis (1997).

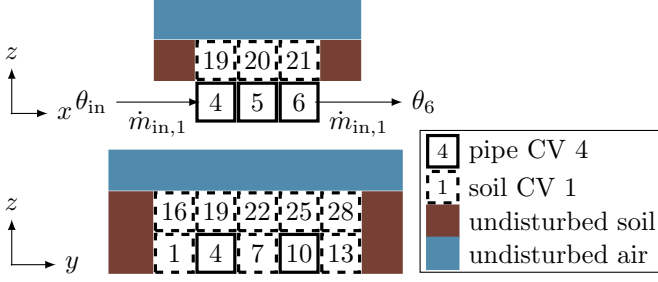


Fig. 3. underground heating system with 30 CVs

If (5) or (6) become infeasible due to the primal variables update, then the primal variables are re-updated by

$$\hat{\mathbf{m}}_k^i = \hat{\mathbf{m}}_k^{i-1} - b\alpha^{i-1}\mathbf{s}^{i-1}, \quad (16)$$

and procedure (16) is repeated with a decreasing $b < 1$ until (5) and (6) are fulfilled. This is similar to the backtracking approach presented by Krishnamoorthy et al. (2019). Engelmann et al. (2025) present a different approach, using relaxation techniques and auxiliary variables to find a feasible α^i .

5. UNDERGROUND HEATING SYSTEM

5.1 System model

To validate the MPC approach and scalability of primal decomposition, we use three versions of a simple underground heating system, commonly applied in underfloor heating and for snow-free surfaces. The versions differ in system size, defined by the number of pipes n_{pi} , control volumes n_{cv} , and CVs per pipe n_x in the x -direction. Figure 3 shows the system with $n_{\text{pi}} = 2$, $n_{\text{cv}} = 30$, and $n_x = 3$. All cases assume two CV layers in the z -direction and soil CVs at both ends in the y -direction. The goal is to minimize energy costs while maintaining soil CV temperatures between 278.15 K and 313.15 K.

System variables The states of the system are the CV temperatures $\boldsymbol{\theta}^\top = [\theta_1 \dots \theta_{n_{\text{cv}}}]$. The algebraic states are the CV mass flows $\dot{\mathbf{m}}^\top = [\dot{m}_1 \dots \dot{m}_{n_x}]$, the pipe pressure losses $\Delta\mathbf{p}^\top = [\Delta p_1 \dots \Delta p_{n_{\text{pi}}}]$, the input temperature of the pipes θ_{in} and the temperature θ_{out} of the mass flow after mixing all pipe exit temperatures (see (20)). The controllable inputs of the system consist of the mass flows in the pipes $\dot{\mathbf{m}}_{\text{in}}^\top = [\dot{m}_{\text{in},1} \dots \dot{m}_{\text{in},n_{\text{cv}}}]$ and the temperature increase $\Delta\theta$ in between pipe out- and input. The uncontrollable inputs are soil temperature θ_s and air temperature θ_a . Table 1 depicts all variables together with their assignment to the vectors contained in \mathcal{V} .

Objective The goal of the controller is to minimize the cost of the required electrical energy for the pumps and the heating system given the electricity price $c_{\text{el},k}$. The cost of electricity for the pumps per time step is given by

$$\dot{j}_{\text{h},k} = \frac{c_{\text{el},k}}{\rho_w \eta_{\text{pu}}} \mathbf{z}_{\text{h},k}^\top \mathbf{u}_{\text{h},k} \quad (17a)$$

with the pump efficiency $\eta_{\text{pu}} = 0.8$. Assuming an electric boiler is used, the cost of the electricity required to heat the water between the pipe inputs and outputs is given by

$$\dot{j}_{\text{t},k} = c_{\text{el},k} c_w u_{\text{t},k} \mathbf{1}_{1 \times n_{\text{pi}}} \mathbf{u}_{\text{h},k}. \quad (17b)$$

Table 1. System variables

states		controllable inputs		uncontrollable inputs		
$\boldsymbol{\theta}$	\mathbf{z}_{h}	\mathbf{z}_{t}	$\dot{\mathbf{m}}$	\mathbf{u}_{h}	\mathbf{u}_{t}	\mathbf{d}
θ_1	Δp_1	θ_{in}	\dot{m}_1	$\dot{m}_{\text{in},1}$		θ_s
\vdots	\vdots	\vdots	\vdots	\vdots	$\Delta\theta$	
$\theta_{n_{\text{cv}}}$	$\Delta p_{n_{\text{pi}}}$	θ_{out}	\dot{m}_{n_x}	$\dot{m}_{\text{in},n_{\text{pi}}}$		θ_a

System dynamics The system dynamics are based on (1) and are not repeated here due to space limitations. The parameters are set to $V = 3.75 \text{ m}^3$, $\sigma_x = 0.025 \text{ W K}^{-1}$, $\sigma_y = \sigma_z = 22.5 \text{ W K}^{-1}$, $\sigma_{\text{pi}} = 44.86 \text{ W K}^{-1}$, $c_w = 4200 \text{ J kg}^{-1} \text{ K}^{-1}$, $\rho_w = 1000 \text{ kg m}^{-3}$, and $c_s \rho_s = 1.5 \times 10^6 \text{ J m}^{-3} \text{ K}$.

Algebraic equations In series with each pipe p , there is a pump that controls the mass flow rate $\dot{m}_{\text{in},p}$. The first set of algebraic equations are the pressure loss relations

$$\Delta p_p(\dot{m}_{\text{in},p}) = \frac{\Delta p_{\text{nom}}}{\dot{m}_{\text{nom}}^2} \dot{m}_{\text{in},p}^2, \quad (18a)$$

where $\Delta p_{\text{nom}} = 8 \times 10^5 \text{ Pa}$ and $\dot{m}_{\text{nom}} = 30 \text{ kg s}^{-1}$ are nominal values. The input temperature is given by

$$\theta_{\text{in}} = \theta_{\text{out}} + \Delta\theta \quad (19)$$

and θ_{out} is governed by

$$\left(\sum_{p=1}^{n_{\text{pi}}} \dot{m}_{\text{in},p} \right) \theta_{\text{out}} = \left(\sum_{p=1}^{n_{\text{pi}}} \dot{m}_{\text{in},p} \theta_{\text{out},p} \right), \quad (20)$$

where $\theta_{\text{out},p}$ is the temperature of the last CV of pipe p , for example θ_6 for $p = 1$ and θ_{12} for $p = 2$ in Figure 3.

5.2 Time discretization

One version of the system was implemented in MATLAB using the time discretization from (3) with a fixed time step of $\Delta t = 2 \text{ h}$, and simulated by solving the resulting equations. A second version, created in DYMOLA with the library from Westphal et al. (2025), also uses backward differentiation but adaptively selects Δt and differentiation order based on the system state. Due to the validated models and advanced discretization, the DYMOLA model serves as the benchmark. Figure 4 compares both simulations, showing the MATLAB model is more accurate for soil CVs (maximum error 0.473 K) than pipe CVs (maximum error 0.936 K) due to slower soil dynamics. Largest pipe deviations occur after increasing $\dot{m}_{\text{in},2}$ from 2 kg s^{-1} to 5 kg s^{-1} at 10 h and decreasing $\Delta\theta$ from 1 K to 0.5 K. Figure 3 shows ambient temperature data; $\dot{m}_{\text{in},1}$ is held constant at 2 kg s^{-1} . For higher accuracy, Δt must be reduced; at $\Delta t = 15 \text{ min}$, the maximum pipe temperature error decreases to 0.23 K.

5.3 Model predictive controllers

Two MPCs were implemented in MATLAB with a control horizon of $n_c = 12$. One solved optimization problem (7) using MATLAB's standard interior-point method (IPM), while the other used the primal decomposition (PD) scheme introduced here with primal variables \mathbf{u}_{h} .

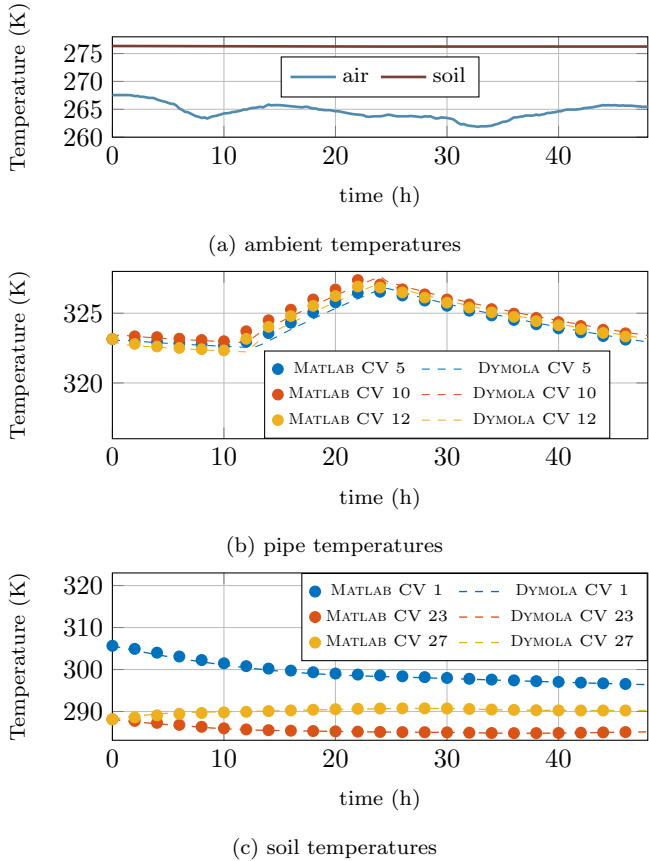


Fig. 4. Comparison of the DYMOLA (dashed lines) and the MATLAB (dots) simulations for the system in Figure 3

Table 2. Numerical results of the two MPCs

number of pipes	number of variables	average $j_h + j_t$ per time step in €		average calc. time per time step in s	
		IPM MPC	PD MPC	IPM MPC	PD MPC
1	19	116.01	117.91	1.18	6.03
2	43	271.53	274.4	12.51	7.81
7	202	1074.7	1298.5	3706	124.29

5.4 Results of the model predictive controller

As shown in Table 2, the IPM outperformed the PD in all three system setups in terms of objective value. However, the PD outperformed the IPM in terms of calculation time for all but the smallest system setup. For $n_{pi} = 2$, the PD MPC calculation time is 62.4% of the IPM MPC calculation time; for $n_{pi} = 7$, it is 3.35%. In conclusion, the PD MPC is more scalable than the IPM MPC. For the two smallest system setups, the average cost per time step is nearly equal for both MPCs, and for the system with seven pipes, the IPM MPC outperforms the PD MPC by 17.2%.

Figure 5 shows the simulation results for the system controlled by the PD MPC. When electricity prices are low, the MPC increases $\Delta\theta$, resulting in higher pipe temperatures. Otherwise, using only the mass flow rate is sufficient for distributing the stored heat at the beginning of the simulation without raising the temperature. As the

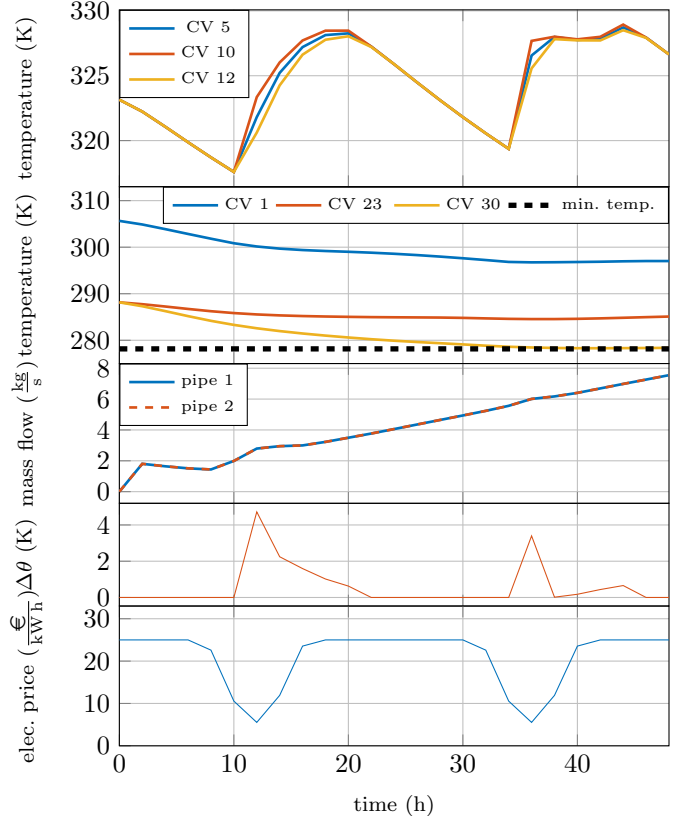


Fig. 5. Primal MPC results for the system in Figure 3

soil temperature decreases, the mass flow increases. Note that the same mass flow is used for both pipes due to the symmetry of the system. The simulation results clearly demonstrate that the PD MPC can control the system according to changing electricity prices and leverage the system's flexibility to minimize operating costs.

5.5 Discussion of the MPC results

Assuming constant fluid properties is common for similar systems (e.g. Maurer et al. (2023)). However, incorporating temperature-dependent fluid properties into the primal decomposition would enhance system accuracy. To fully evaluate the benefits of primal decomposition, more advanced system setups that account for uncertainty in predictions are required. Additionally, a detailed analysis of control quality and convergence guarantees concerning the time step Δt and control horizon is necessary.

6. CONCLUSION

This work presents a direct method for model predictive controller design for thermo-hydraulic systems modeled by control volumes. Using primal-decomposition increases the approach's scalability massively compared to a standard MPC approach. Future work should include a more extensive analysis of more sophisticated system setups to provide a more robust evaluation of the presented approach. Additionally, comparisons with other automated MPC frameworks, as presented in Houska et al. (2011) and Chen et al. (2019), are necessary.

DECLARATION OF GENERATIVE AI AND AI-ASSISTED TECHNOLOGIES IN THE WRITING PROCESS

During the preparation of this work the authors used DeepL Write and GPT4.1-Mini in order to improve readability. After using these tools, the authors reviewed and edited the content as needed and take full responsibility for the content of the publication.

REFERENCES

- Alikhani, J., Shoghli, B., Bhowmik, U.K., and Massoudieh, A. (2016). An Adaptive Time-Step Backward Differentiation Algorithm to Solve Stiff Ordinary Differential Equations: Application to Solve Activated Sludge Models. *American Journal of Computational Mathematics*, 6(4), 298–312. doi:10.4236/ajcm.2016.64031.
- Benonysson, A. (1991). *Dynamic modelling and operational optimization of district heating systems*.
- Bertsekas, D.P. and Tsitsiklis, J.N. (1997). *Gradient Convergence in Gradient Methods*.
- Boyd, S. (2014). *Subgradient Methods*.
- Boyd, S., Xiao, L., Mutapcic, A., and Mattingley, J. (2008). *Notes on Decomposition Methods*.
- Chen, Y., Bruschetta, M., Picotti, E., and Beghi, A. (2019). MATMPC - A MATLAB Based Toolbox for Real-time Nonlinear Model Predictive Control. In *2019 18th European Control Conference (ECC)*, 3365–3370. doi:10.23919/ECC.2019.8795788.
- Deng, N., Cai, R., Gao, Y., Zhou, Z., He, G., Liu, D., and Zhang, A. (2017). A MINLP model of optimal scheduling for a district heating and cooling system: A case study of an energy station in Tianjin. *Energy*, 141, 1750–1763. doi:10.1016/j.energy.2017.10.130.
- Engelmann, A., Shin, S., Pacaud, F., and Zavala, V.M. (2025). Scalable Primal Decomposition Schemes for Large-Scale Infrastructure Networks. *IEEE Transactions on Control of Network Systems*, 12(2), 1687–1698. doi:10.1109/TCNS.2025.3526709.
- European Commission (2019). *The European Green Deal*. Technical report, Brussels.
- Fabien, B.C. (2010). dsoa: The implementation of a dynamic system optimization algorithm. *Optimal Control Applications and Methods*, 31(3), 231–247. doi:10.1002/oca.898.
- Fraunhofer ISE (2021). *Wege zu einem klimaneutralen Energiesystem*. Technical report.
- Frey, J., Baumgärtner, K., and Diehl, M. (2024). Gauss–Newton Runge–Kutta integration for efficient discretization of optimal control problems with long horizons and least-squares costs. *European Journal of Control*, 80, 101038. doi:10.1016/j.ejcon.2024.101038.
- Herty, M., Pareschi, L., and Steffensen, S. (2013). Implicit–Explicit Runge–Kutta Schemes for Numerical Discretization of Optimal Control Problems. *SIAM Journal on Numerical Analysis*, 51(4), 1875–1899. doi:10.1137/120865045. Publisher: Society for Industrial and Applied Mathematics.
- Houska, B., Ferreau, H.J., and Diehl, M. (2011). ACADO toolkit—An open-source framework for automatic control and dynamic optimization. *Optimal Control Applications and Methods*, 32(3), 298–312. doi:10.1002/oca.939.
- IEA (2018). *The Future of Cooling*. Technical report, IEA, Paris.
- Kazantzis, N. and Kravaris, C. (1999). Time-discretization of nonlinear control systems via Taylor methods. *Computers & Chemical Engineering*, 23(6), 763–784. doi:10.1016/S0098-1354(99)00007-1.
- Krishnamoorthy, D., Foss, B., and Skogestad, S. (2019). A Primal decomposition algorithm for distributed multistage scenario model predictive control. *Journal of Process Control*, 81, 162–171. doi:10.1016/j.jprocont.2019.02.003.
- Lund, H., Möller, B., Mathiesen, B.V., and Dyrelund, A. (2010). The role of district heating in future renewable energy systems. *Energy*, 35(3), 1381–1390. doi:10.1016/j.energy.2009.11.023.
- Lund, H., Werner, S., Wiltshire, R., Svendsen, S., Thorsen, J.E., Hvelplund, F., and Mathiesen, B.V. (2014). 4th Generation District Heating (4GDH): Integrating smart thermal grids into future sustainable energy systems. *Energy*, 68, 1–11. doi:10.1016/j.energy.2014.02.089.
- Maurer, J., Ratzel, O.M., Malan, A.J., and Hohmann, S. (2021). Comparison of discrete dynamic pipeline models for operational optimization of District Heating Networks. *Energy Reports*, 7, 244–253. doi:10.1016/j.egyr.2021.08.150.
- Maurer, J., Tschuch, N., Krebs, S., Bhattacharya, K., Cañizares, C., and Hohmann, S. (2023). Toward transactive control of coupled electric power and district heating networks. *Applied Energy*, 332, 120460. doi:10.1016/j.apenergy.2022.120460.
- Olanrewaju, O.I. and Maciejowski, J.M. (2017). Implications of discretization on dissipativity and economic model predictive control. *Journal of Process Control*, 49, 1–8. doi:10.1016/j.jprocont.2016.11.002.
- Palomar, D. and Chiang, M. (2006). A tutorial on decomposition methods for network utility maximization. *IEEE Journal on Selected Areas in Communications*, 24(8), 1439–1451. doi:10.1109/JSAC.2006.879350.
- Taheri, S., Hosseini, P., and Razban, A. (2022). Model predictive control of heating, ventilation, and air conditioning (HVAC) systems: A state-of-the-art review. *Journal of Building Engineering*, 60, 105067. doi:10.1016/j.jobee.2022.105067.
- Vaclavek, P. and Blaha, P. (2013). PMSM model discretization for Model Predictive Control algorithms. In *Proceedings of the 2013 IEEE/SICE International Symposium on System Integration*, 13–18. IEEE, Kobe, Japan. doi:10.1109/SII.2013.6776649.
- Vieth, J., Westphal, J., and Speerforck, A. (2025). District heating network topology optimization and optimal co-planning using dynamic simulations. *Advances in Applied Energy*, 19, 100233. doi:10.1016/j.adapen.2025.100233.
- Wack, Y., Baelmans, M., Salenbien, R., and Blommaert, M. (2023). Economic topology optimization of District Heating Networks using a pipe penalization approach. *Energy*, 264, 126161. doi:10.1016/j.energy.2022.126161.
- Westphal, J., Brunnemann, J., and Speerforck, A. (2025). Enabling the dynamic simulation of an unaggregated, meshed district heating network with several thousand substations. *Energy*, 135434. doi:https://doi.org/10.1016/j.energy.2025.135434.